치의과학석사 학위논문

Biomechanical and preclinical study of the separable dental implant fixture

분리형 치과 임플란트 식립체의 생역학 및 전임상 평가

2019년 2월

서울대학교 대학원

치의과학과 구강악안면외과학 전공

정주희 (Joohee Jeong)

Biomechanical and preclinical study of the separable dental implant fixture

분리형 치과 임플란트 식립체의 생역학 및 전임상 평가

지도교수 이종호

이 논문을 치의과학석사 학위논문으로 제출함

2018년 10월

서울대학교 대학원

치의과학과 구강악안면외과학 전공

정주희 (Joohee Jeong)

정주희(Joohee Jeong)의 **석사학위논문을 인준함**

2018년 12월

위 원 장 김성민 (인)

부위원장 김봉주 (인)

위 원 이종호 (인)

Abstract

Biomechanical and preclinical study of the separable dental implant fixture

Joohee Jeong, DDS

Program in Oral and Maxillofacial Surgery, Department of Dental Science,

Graduate School, Seoul National University

(Directed by Professor Jong-Ho Lee, DDS, MSD, PhD)

Purpose

Peri-implantitis is managed by various methods including chemical and mechanical treatments such as local or systemic antibiotics, ultrasonic cleansing, and debridement. However, it is not always effective. Hence, separable dental implant fixture was newly designed for easy management of progressive peri-implantitis by changing the infected top fixture part. The purpose of this study is to assess the biomechanical stability and osseointegration parameters of newly designed separable implant and compare the outcomes with conventional non-separable implant for the feasibility of clinical application.

Materials and Methods

Newly designed separable fixture is conceptualized to be separable into two parts (upper and lower) for an easy replacement after alveolar bone loss, which is modified from conventional one-piece fixture. The exterior design of conventional and separable fixture is identical, which is 6 mm in length, 3.4 mm in diameter. A finite element model was constructed for biomechanical study of both implant types. The applied loads were 100N vertically, 100N at 15 degrees, and 30N at 45 degrees. The peak von Mises stress (PVMS) was measured for comparative analysis. In preclinical study, a total of forty rabbits received two separable fixtures at left tibia, while two non-separable fixtures at right tibia. They were sacrificed after 3 or 6 weeks of healing, and the implant specimens were evaluated by resonance frequency analysis, CT, removal torque test, histopathology and histomorphometric analysis.

Results

In the biomechanical study with finite element model, newly designed separable implant showed higher stress than non-separable implant in vertical load, but it was considered that stress concentration on the cortical bone could be reduced as the stress was well distributed in the cancellous bone in separable implant compared to non-separable implant. Moreover, separable implant was more excellent in load distribution and stress transfer within the bone at oblique load, so it was confirmed to have lower stress compared to non-separable implant.

In the preclinical study with rabbit tibia model, there was no significant difference in implant stability and bone volume fraction depending on implant type. By the way, greater values of removal torque were observed in separable implant in relation to the control. It could most likely be attributed to new bone adhesion in the gap of a separable

fixture. This study demonstrated no significant different or greater results for separable implant when compared with conventional non-separable implant. Based on this evaluation, separable implant is scientifically documented and the results suggest that separable implant has sufficient osseointegration and biomechanical stability.

In conclusion, there is a feasibility of clinical application of separable dental implant fixture based on the osseointegration and biomechanical stability in this study.

Key words: separable fixture, dental implant, biomechanical, osseointegration, stability

Student number: 2017-22467

Table of Contents

I. Introduction

The use of dental implant is significantly increased due to high success rate with advanced technique over the past decades. With the increased use of implants, peri-implant inflammatory conditions are frequent in the dental implanted population and prevalence of peri-implantitis has been reviewed. Peri-implantitis is a site-specific infectious disease which causes an inflammatory reaction with loss of supporting bone surrounding an osseointegrated implant. Prevalence of peri-implantitis was reported as 5~8% in selected implant systems[1], and 21.7 % (95% CI 14~30) in the meta-analysis as weighted mean value by Derks and Tomasi[2]. Atieh et al. reported prevalence of peri-implantitis was 18.8 % (95 % CI 16.8~20.8) and the patients with a history of periodontitis were estimated to have an incidence of peri-implantitis as 21.1 % (95% CI 14.5~27.8) in a subgroup analysis[3]. So, peri-implantitis poses a challenge to a long term success of implant osseointegration for a stable masticatory function. The etiology of peri-implantitis has a lot in common with periodontitis. Peri-implantitis, like periodontitis, is a multifactorial disease characterized by an imbalance in oral microflora and host immunity system, which eventually results in a destructive inflammatory process[4]. Risk factors are considered to include microbiological factors, inflammation, diabetes, smoking, systemic diseases, and genetic factors for the progress of peri-implantitis[4,5]. The microenvironment of peri-implant gingival sulcus is favorable to specific micro bacteria which are considered key pathogens triggering inflammatory reaction leading to pathology[4]. Gram-negative anaerobic bacteria ascertained common to peri-implantitis include Aggregatibacter actinomycetemcomitans, Porphyromonas gingivalis, Tannerella forsythia, and the like[4].

Peri-implantitis is managed by various methods including chemical and mechanical treatments such as local or systemic antibiotics, ultrasonic cleansing, and

debridement, however, it is not always effective. The optimal treatment of peri-implantitis is a regeneration of the lost supporting alveolar bone around an implant (re-osseointegration). Attempts have been made over the past 20 years to resolve peri-implantitis, but standard treatment protocol of peri-implantitis has not been established[6]. A new dental implant fixture which is separable for easy retrieval of the top part in case with peri-implantitis was designed. When progressive peri-implantitis induced alveolar bone loss occurs and a fixture is exposed, only the exposed upper part of the separable fixture can be removed and replaced by a new one while the sound lower part of the fixture maintained. So that the bacterial infection which is a major cause of peri-implantitis can be removed mechanically and the entire recovery can be achieved. It must effectively treat progressed peri-implantitis by changing the infected top part of the fixture with easily relieving the inflammation. The modification of fixture with separable design can thus bring advantage to the response of peri-implant bone, accelerating the healing process and improving new bone formation.

Differences may exist between separable and non-separable implants with different designs. Proper evaluation of a new implant including biomechanical stability and in vivo osseointegration study is mandatory prior to clinical application. The purpose of this experiment was to compare stability and osseointegration of a newly designed separable implant with that of a conventional non-separable implant to assess the feasibility of separable dental implant fixture for human application.

II. Materials and Methods

1. Biomechanical study in finite element and synthetic bone model

1.1 Finite element model

Implant systems including fixture, abutment, and abutment screw of two groups were designed to a 3-dimensional computer aided design (CAD) model using Solidworks software (Solidworks 2016, Dassault systems, France). A crown model was constructed corresponding to the first molar of cone beam computed tomography (CBCT) images.

To compare stress distribution and biomechanical stability within bones between the two groups, CBCT images of normal Korean female adult skulls were obtained with 0.25 mm thickness cuts. The obtained 2-dimentional images were used to reconstruct 3D mandible model using Mimics program (Mimics research v.19.0, Materialise, Belgium). Previous literature reported that bite force is mainly loaded in the first molar during mastication, hence, this study constructed a single tooth model by extracting the portion corresponding to the first molar[7]. A shape of the bone was reproduced as distinguished cortical and cancellous bone, and the cortical bone was constructed to have a uniform thickness of 2 mm with reference to previous literature (Figure 1. A)[8].

Three-dimensional CAD models of bone and implant including fixture, abutment, abutment screw, and crown were prepared in Solidworks software. A finite element analysis program (Abaqus CAE 2016, Dassault systems, France) was used to assemble the bone and implant to construct single tooth surgical model (Figure 1), and Hypermesh program (Altair hyperworks v.17.0, Altair engineering, USA) was used to form mesh in the model. The properties of implant, crown, and bone were applied referring to previous literature (Table 1)[9-13].

A complete restraint of six degrees of freedom (DOF) which is an axial and rotational movement of x, y, z was applied so that the cortical and cancellous bone were not moved or rotated at all in three dimensions (Figure 1. B). The interfaces of cortical and cancellous bone, bones and fixture, and abutment and crown were applied “tie contact” assuming complete adhesion. The interfaces between fixture, abutment, and abutment screw were applied “general contact” assuming friction. A friction coefficient of 0.5 was used[11].

1.2 Finite element analysis

Finite element models were constructed for analysis of conventional non-separable and separable implant. The mechanical properties were applied as per previous literatures (Table 1)[9-13]. A preload of 200N was applied vertically to an abutment screw to assume the condition of fixation between the abutment and fixture[11]. After which, considering loads generated at various angles in the oral cavity, the load of 100N vertically[14], 100N at 15 degrees[14], and 30N at 45 degrees[15] were applied at first molar (Figure 1). Peak von Mises stress (PVMS) of the cortical and cancellous bone and the implant (fixture, abutment, and abutment screw) were measured to compare biomechanical stability between the two groups.

1.3 Implant stability test in synthetic bone model

Implant stability was tested to compare biomechanical stability between the two groups by installing separable and non-separable implants in synthetic bone models (Generic slice PR0013, Synbone AG, Switzerland). Three different sized holes (Ø2.2, 2.8,

3.3 mm) were made and the fixtures were inserted at each hole in synthetic bone models (n=72) (Figure 2). Holes were drilled with initial (pilot drill), intermediate and final (Ø2.2, 2.8, 3.3 mm drill) rotary instruments (Straumann Surgical Cassette, Straumann, Switzerland). The fixture was installed by drilling (10rpm, 30Ncm) at first and the final installation was done manually by torque wrench (30Ncm). The implants were placed at bone level.

Resonance frequency analysis (RFA) was performed using the Osstell mentor (Integration Diagnostics AB, Sweden). A standardized abutment, SmartPeg (Integration Diagnostics AB, Sweden) was screwed into a fixture using a SmartPeg mount by tightening with 3 fingers forces, approximately 4-6 Ncm torque. Subsequently, a transducer probe (Osstell mentor probe) was held close to the SmartPeg but contactless so that the probe tip pointed at small magnet on the top of the SmartPeg with a distance of 2–3 mm during pulsing time. The measurements were repeated six times from all quarters respectively (Figure 2). Then the mean of each sample was calculated to minimize measurement errors.

2. Preclinical study in rabbit tibia model

2.1 Fixture preparation

Two groups of SLA surfaced implant fixtures were prepared: separable fixture (2 pieces) and non-separable fixture (1 piece). Separable implants were used as an experimental group, while conventional non-separable implants of the same exterior shape but one piece were used as a control group. The designs and dimensions of separable and non-separable implants were same as the CAD model. The fixtures with

dimensions of 6.0mm in length and 3.4mm in outer diameter, with a screw thread pitch of 0.4mm and a thread depth of 0.47mm, and with three self-threading cutting edges in apical portion to reduce insertion torque and to increase drilling capacity were prepared. The exterior design of separable and non-separable implant was identical. The separable implant had a standard hex on top of the bottom part of the fixture and it was characterized by a passive fit with the top part of the fixture. External hex type of the bottom part and internal hex type of the top part were fit and separable passively (Figure 3. A, Figure 4. A).

Implants were manufactured with titanium grade5 ELI (Ti-6Al-4V extra low interstitial elements) by a milling machine (Cincom L20, Citizen Machinery Co. Ltd., Japan). They were washed with distilled water, dried, and treated with sandblasted, large grit, acid-etched (SLA) surface. All implants for the animal experiment were packaged and sterilized in ethylene oxide (EO) gas prior to animal surgery. A total of 160 implants, eighty separable and non-separable implants for each, were ready with the same care used for commercial products (Figure 3) (Implanova Co. Ltd., Republic of Korea).

2.2 Approval for animal research

This study was conducted at the Laboratory Animal Resource Center of Dental Research Institute in Seoul National University and was approved by the Seoul National University Institutional Animal Care and Use Committee (IACUC). Ethical clearance for in vivo experiment was obtained from the IACUC prior to the experimental procedure (SNU_1712222).

2.3 Animal surgery

A total of forty 11~17 weeks old male New Zealand white rabbits (Oryctolagus cuniculus) (2.52-2.88 kg in weight) were used. Two separable fixtures (2 pieces) were installed in left tibia and two non-separable fixtures (1 piece) were installed in right tibia.

Preoperatively, body weights of the rabbits were measured and cefazolin, 20 mg/kg, IV (Cefozol, Hankook Korus Pharm., Republic of Korea) was administered as a prophylactic antibiotic. The rabbits had temperance in eating at least 12 hours before general anesthesia. General anesthesia was induced intravenously via marginal veins of ear with a mixture of xylazine (Rompun, 20 mg/ml, Bayer AG, Germany) and tiletamine-zolazepam (Zoletil, 50 mg/ml, Virbac, France) (1:1 volume, dosage 0.1ml/kg) and maintained (1:1 volume, dosage 0.05 ml/kg) during the surgery.

The rear legs of the rabbits were shaved at the surgical sites and remaining hairs of the other sites were covered by bandage before transferring to an operating room. The rabbits were put in a supine position and surgical sites were washed with povidone-iodine (Betadine solution, Korea Pharma, Republic of Korea) and draped with sterile towel. Principles of sterile surgical techniques were applied during surgery.

After 1ml of local anesthetic (2% lidocaine with 1:100,000 epinephrine, 1.8ml, Yuhan, Republic of Korea) was infiltrated subcutaneously for hemostasis, a skin incision was made with a periosteal flap to expose each proximal tibia. The proximal tibial metaphysis was exposed with minimal damage to the surrounding soft tissue including muscles. Tendons were preserved intact.

Proximal epiphysis of rabbit tibia has a wide medial face that is devoid of muscle insertion and slightly convex, which is suitable for an implant installation. The surface on

median aspect of the proximal tibia was checked to determine the implant location. The space between the anterior border and the median border of the medial condyle was selected for implant placement. As the location of implant in tibia may influence osseointegration due to different bone features from epiphysis to diaphysis, in this study the implants were located in sponge bone so the whole fixture surface had similar characteristics of contact bone. Two fixtures were positioned on the medial surface of tibial medial condyle, so the fixtures were installed in sponge bone, not into a marrow cavity. One fixture was positioned anteriorly and the other was positioned posteriorly of the tibial medial condyle with a 8mm gap between the fixtures (Figure 5).

Holes were drilled with initial (lance drill), intermediate (Ø2.2 mm, twist drill), and final (Ø3.0 mm, twist drill) rotary instruments under copious sterile saline irrigation (Taper KIT, OTSK, Osstem, Republic of Korea) (Implantmed, W&H, Austria). A fixture was inserted by drilling (10rpm, 30Ncm) at first and final installation was done manually by torque wrench (20Ncm). The implants were positioned at bone level, at the same level with respect to the marginal bone, and fixed mono-cortically. Two implants from each group were inserted into each tibia, total 4 implants in a rabbit.

Immediately after implant placement, initial (primary) implant stability was measured four times per an implant from two different directions with Osstell instrument (Osstell ISQ, Integration Diagnostics AB, Sweden) for RFA. Following application of cover screw, the elevated flaps were repositioned and closed with continuous sutures with 4-0 Blue Nylon (Ailee Co., Ltd., Republic of Korea). In all, forty New Zealand white rabbits received a total of 160 implants (n=80 per group) in their tibia, all of which were examined by RFA and digital x-rays.

Radiographic images were taken by using C-arm (Arcadis Varic, Siemens Co.,

Germany) immediately after the surgery and post-operatively once a week until sacrifice. An implant was irradiated with x-ray perpendicularly to the fixture so that the fixture threads are shown clearly.

Postoperatively, cefazolin, 20 mg/kg, IV was administered twice a day for three days as a prophylactic antibiotic. Each rabbit was housed in an individual cage with 12h cycles of light in controlled temperature (21°C). They were fed and watered ad libitum. There was no activity restriction and no supportive orthotic devices used postoperatively. Forty rabbits successfully underwent surgery. Rabbits were observed daily for inflammation, wound dehiscence, infection, and general health.

Separation of a separable fixture did not occur during the fixture installation in the tibia. All rabbits showed appropriate healing and no complications occurred such as tibial fracture, wound dehiscence, and infections at the operation sites during the postoperative period. The soft tissue seal and hard tissue osseointegration resulted in the good healing process, showing the initial success of the implant. The rabbits recovered normal activity after surgery.

2.4 Resonance frequency analysis (RFA)

All rabbits were applied for RFA to evaluate implant stability. And RFA was performed using Osstell ISQ. A standardized abutment, SmartPeg was screwed into a fixture with a SmartPeg mount by tightening with 3 fingers forces, approximately 4-6 Ncm torque. Subsequently, a transducer probe (Osstell ISQ Probe II) was held close to the SmartPeg but contactless so that the probe tip pointed at small magnet on the top of the SmartPeg with a distance of 2–3 mm during the pulsing time. The probe should be

held stable until the instrument makes beep alarm and displays ISQ. The double measurements were repeated in two directions, proximal to distal and lateral to medial, in each implant, respectively. Then mean of each sample was calculated to minimize measurement errors. After 3 or 6 weeks of the healing period, ISQ was measured again in the same way at the time of sacrifice of the rabbits.

2.5 Animal sacrifice

Twenty randomly selected rabbits were sacrificed at 3 or 6 weeks after implantation. All animals were euthanized with an intramuscular overdose of succinylcholine (Succicholine, Ilsung Pharmacy, Republic of Korea), 0.1 mL/kg, after general anesthesia induced intravenously via marginal veins of the ear with a mixture of xylazine and tiletamine-zolazepam (1:1 volume, dosage 0.1ml/kg).

Immediately after sacrifice, soft tissues including periosteum of the tibia were removed to expose the integrated implants. Following removal of cover screws, secondary implant stability was measured using Osstell ISQ. When required, the overgrown bone was flattened to remove a cover screw with sterile physiologic saline using standard drills in the implant kit.

Subsequently, the tibia specimens containing fixtures were harvested en bloc using an electric saw and fixated in 10% neutral buffered formalin (pH 6.8-7.2, BBC Biochemical, WA, USA) in cold storage for further tests. The tibia specimens were prepared with about 0.5cm safety bone margin from the fixture using a cutting system (Exakt 300 CP, Exakt Technologies, OK, USA) following a week of fixation. Consequently, the implant specimens were evaluated by RFA, micro computed

tomography (μCT), removal torque test, histology and histomorphometric analysis.

2.6 Bone volume fraction (BVF, BV/TV) in micro computed tomographic study

All specimens were scanned with a high-resolution CT system (SkyScan1173 Ver.1.6, SkyScan, Belgium) at a spatial resolution of 9.945 μm (voxel dimension). We used a source voltage and current of 130 kV and 60 μA and a 1.0 mm Aluminum filter. Further, we used an exposure time of 500 ms, a frame averaging of 4 and a rotation step of 0.3°. This resulted in an image pixel size of 9.945 μm. The section reconstruction was performed using reconstruction program (Nrecon Ver.1.7.0.4, Bruker, Belgium). For each specimen, a total of 2240 consecutive micro tomographic slices were acquired.

Quantitative analysis of the new bone formation around implants was carried out. Parameters such as bone volume fraction (BVF, BV/TV, bone volume to total volume ratio) and bone volume (BV) were directly calculated in the volume of interest (VOI) from the 2D and 3D datasets using CTAn software (CT analyser v.1.17, Bruker, Belgium). Bone volume fraction is used to evaluate relative changes in bone volume density. After μCT scans, the specimens were divided into two groups for histological evaluation or removal torque test.

2.7 Removal torque test

The tibia implant specimens were used for biomechanical evaluation with removal torque test in a random balanced fashion. Removal torque test was performed to evaluate shear strength of bone-implant interface for both implant types by applying a counterclockwise rotation to implant axis. Peak resistance values of reverse torque

rotation when uninstalling the implants from the tibia specimens were measured automatically using a digital torque gauge (MTT03-100, Mark-10, NY, USA). An axis of the torque gauze device was aligned to an axis of an implant with mount to apply axial moments in test (Figure 6). For this reason, a mount drill fixed to the device was first attached to a mount which is tightened in a fixture, thereby guaranteeing the alignment of implant and device. The manufactured mount drill with a square shape that fits precisely onto the head of an implant mount was used. After the digital torque gauge was connected to the mount with the fixture, rotation rate of reverse torque was applied until the fixation of the bone-implant interface was loosened. The peak reverse torque values required for a complete loosening of the implants, which was assumed to be removal (failure) torque of the bone-implant interface, were recorded.

2.8 Histology and histomorphometric analysis

Peri-implant bone regeneration was assessed histomorphometrically with percent bone implant contact (%BIC) and percent bone density (%BD) at 3 or 6 weeks after implantation. The fixated specimens were dehydrated in a graded ethanol series, in 70%, 90%, 95%, and 100% ethanol, using a dehydration system with agitation and a vacuum, and were infiltrated and embedded in light-curing methacrylate (Technovit 7200 VLC, Heraeus Kulzer, Germany) to produce undecalcified sections. The implants were cut and grinded approximately 50 um thick along a longitudinal plane by a sawing and grinding machine (Exakt 400CS, Exakt Technologies, OK, USA). Specimens were stained with hematoxylin and eosin (H&E) to evaluate new bone formation around the fixtures under a light microscope. All representative specimens underwent histologic evaluation with a light microscope (Olympus BX, Olympus, Japan) connected to a computer. All the

measurements were calculated under 100× magnification. A higher magnification and zoom were used to help determine whether or not the bone.

2.9 Statistics

The separable implants were compared with the non-separable implants according to the results from resonance frequency analysis, μCT, and removal torque test. Statistical analysis was performed using a commercially available software program (IBM SPSS Statistics v22.0, IBM Corporation, NY, USA). Continuous variable data were presented as mean and standard deviation. Normality assumption and equality of variance were checked. Normal distribution of removal torque values was evaluated with Kolmogorov-Smirnov test and Shapiro-Wilk test due to sample size. Multiple comparisons for ISQ, bone volume fraction of μCT, and removal torque values were conducted using two-way analysis of variance (ANOVA) and post-hoc Bonferroni tests to compare the mean and to investigate possible effects of fixture type (separable and non-separable) and healing period (3 or 6 weeks). In conclusion, two-way ANOVA was performed to verify the main effects of fixture type and healing period on ISQ, % bone volume fraction, and removal torque values and their interaction effects. All values were considered statistically significant when p-value was less than 0.050.

III. Results

1. Biomechanical study in finite element and synthetic bone model

1.1 Designs and dimensions of separable and non-separable implants

So far, conventional structure of one-piece fixture was used for partial or fully edentulous patients (Figure 4. B). But this classical implant system is reported to be failed in the long term in case of peri-implantitis. Therefore, the newly designed separable fixture was introduced to treat peri-implantitis and improve the success rate of the implant in long term (Figure 4. A). As shown in Figure 4A, a separable fixture which is modified from the non-separable one-piece fixture is able to be separated into two parts (upper and lower parts) for an easy replacement after an alveolar bone loss.

Size of the separable fixture is identical with the conventional non-separable fixture, which is 6 mm in length, 3.4 mm in diameter, and 0.4 mm of screw thread pitch. Therefore, it is possible to apply same abutment and abutment screw of which head diameter is 2.5 mm, body diameter 1.6 mm, length 7.5 mm for both separable and non-separable implant (Figure 5C). This system was designed to be able to replace implant fixture efficiently after loss of alveolar bone in case of peri-implantitis.

1.2 Von Mises stress distribution with finite element analysis

To investigate stress distribution and biomechanical stability within bones between classical non-separable implant and new designed separable implant, Hypermesh program was used to form mesh in the finite element model. The number of elements and nodes in the model was shown in Table 2.

The preload applied to abutment screw fixed the connection between fixture and abutment, and it was confirmed that stress distribution was concentrated on the abutment screw when only preload was applied. This way, excess stress applied on the abutment

screw is considered to result in fatigue fracture of the abutment screw if load is applied at various directions long time.

Figure 7-8 shows stress distribution on the implants and surrounding tissues under various loading and analysis conditions. As shown in figure 7-8, stress is more concentrated on the cortical bone than cancellous bone. Under vertical loading condition, stress was highest at the junction of fixture and abutment screw as it is mainly contacted connecting region between the fixture and abutment screw (Figure 7). On the other hand, if the load was applied diagonally or sideways at oblique load, then stress was highest at the region of bending load applied between fixture and abutment (Figure 8). Yang[16] reported that implant structure and loading conditions affect stress distribution on the tissues around an implant, and it was also confirmed in this study that the pattern of stress distribution differs according to loading conditions.

The PVMS values of implants and surrounding tissues were compared (Table 3, 4). The PVMS value of cortical bone was around 26% higher in separable implant (138MPa) than non-separable implant (109MPa) under vertical loading condition, but at oblique load separable implant was around 16% (15°), 20% (45°) lower than non-separable implant (Table 3). In cancellous bone, separable implant generated higher stress than non-separable implant at all loading conditions (Table 3). Similar to stress distribution of bones, the PVMS values of the implant (fixture, abutment, and abutment screw) were higher in separable implant than non-separable implant at vertical loading condition, but non-separable implant was rather higher than separable implant at oblique load (Table 4). In particular, the difference in stress between the two groups was significant at oblique load, and the stress values of non-separable fixture were higher than the yield strength (552 MPa) of Titanium grade 4 (Table 4).

As a fixture is separated in the separable implant, stress was appropriately distributed on the two structures so that stress is not excessively concentrated on the abutment or its screw. The PVMS values of abutment screw were significantly lower in separable implant than in non-separable implant under oblique load, and it means a possibility of abutment screw fatigue fracture inside the fixture is lower in the separable implant. Moreover, stress was transferred more desirably to the cancellous bone in separable implant than in non-separable implant, and it may reduce stress concentration in cortical bone.

1.3 Implant stability in synthetic bone model

RFA was performed according to the different sized implant holes (Ø2.2, 2.8, 3.3 mm) between two groups. Separable implant showed higher ISQ than non-separable implant and all results show reasonable stability greater than 60 (Figure 9). Implant failure is regarded if initial ISQ value is less than 60 in reference of Osstell guideline[17]. Mean ISQ of each group is summarized in Table 5. One-way ANOVA showed that ISQ was not significantly different in Ø2.2 and 2.8 mm sized holes between separable and non-separable implants. But separable implants (76.0 ± 2.2) showed higher ISQ than non-separable implants (71.0 ± 4.5) in Ø3.3 mm sized holes with significant differences ($p=0.0146$) (Figure 9).

2. Preclinical study in rabbit tibia model

2.1 Radiological findings

All fixtures were retained well on the tibias. Bone loss around the fixture threads

did not occur. Weekly x-ray images showed nothing special such as overt fractures. Although new bone engagement between the micro gap of separable fixture was found on μCT images, this gap was not found in conventional X-ray images. On μCT, there were some cases in which periosteal new bone formation was found around the cover screw.

2.2 Resonance frequency analysis (RFA)

Mean ISQ of each group is summarized in Table 6. Within each healing period, non-separable implants showed higher ISQ than separable implants without statistically significant differences (Figure 10). And no significant differences between separable and non-separable implants were confirmed ($F=3.67$, $p=0.057$). Two-way ANOVA showed that the main effect of healing period on ISQ was significant ($F=68.74$, $p=0.000$). The mean ISQ of 6 weeks healing (62.84 ± 0.29) was 6.15 percent higher than that of 3 weeks healing (59.20 ± 0.33) in both types of implants ($p=0.000$), with no significant difference between the fixtures. There was no significant interaction effect ($F=0.98$, $p=0.324$).

2.3 Bone volume fraction (BVF, BV/TV) in micro computed tomographic study

From the resulting voxel data, a cylindrical VOI with a resolution of 9.945 μm included 0.8 mm around the fixture with a height of 0.9mm from the external platform shoulder of the lower part of a separable fixture, which was matched up with the location and area of VOI in a non-separable fixture (243 cuts; number of layers) (Figure11. A). Furthermore, 3D images of the trabecular bone structures around the implant could be generated using CTvox program (CTvox, Bruker, Belgium) and bone-implant surfaces,

new bone formation, and osseointegration around the micro gap of a separable fixture were observed (Figure 11. B).

Two-dimensional μCT view analysis revealed new bone formation between the gap of separable fixture compared to the non-separable fixture. Three-dimensional μCT reconstructions indicated increased trabecular bone formation occurred around the fixtures. Mean BVF of each group is summarized in the Table 7. Within each healing period, non-separable implants showed higher BVF than separable implants without statistically significant differences (Figure 12). And no significant differences between separable and non-separable implants were confirmed ($F=1.67$, $p=0.198$). In comparing BVF with different healing period, mean BVF in 3 weeks of healing (50.43 ± 0.56) was 10.09 percent higher than that in 6 weeks of healing (45.81 ± 0.52) with significant statistic differences ($F=36.38$, $p=0.000$). The interaction effect was not significant at 0.050 levels ($F=0.70$, $p=0.404$).

2.4 Removal torque value (RTV)

The main effect of fixture type on RTV was significant ($F=16.40$, $p=0.000$). So there is a significant difference in mean RTV according to the fixture type, and separable implant (25.65 ± 1.95) shows a greater mean RTV than non-separable implant (13.63 ± 2.24) (Figure 13). There is no significant difference in RTV depending on the healing period ($F=0.81$, $p=0.374$). The interaction effect was not significant at 0.050 levels ($F=0.00$, $p=0.953$). A summary of all statistics for both implant types at two different healing periods is shown in Table 8.

2.5 Histology and histomorphometric analysis

A software (Kappa image base metro, Kappa Opto-Electronics, Germany) was used to measure the %BIC which was calculated as the length ratio of bone surface in direct contact with intra-bony implant surface and %BD which was the percentage of new bone formation area ratio inside threads within region of interest (ROI) (Figure 14). The upper threads area was included in %BIC but the apical area was excluded in %BIC.

Histologically four representative specimens of each group showed no prominent inflammation or soft tissue involvement between the bone and the fixture. But bone engagement between the micro gaps of the separable fixture was found (Figure 15). Analyzing the histological images of both implants in two different healing period proposed that in the early ones (3 weeks of healing) the new bone formed around the implants is not much mineralized and a smaller osteoid surface of the regenerated bone is shown, while in the later ones (6 weeks of healing) the new bone is more mineralized. All ground sections showed osteoid in woven bone around the fixture, which suggested new bone formation in H&E stained images. The fixtures were predominantly in contact with marginal cortical bone along the upper edge of the fixture and in tight contact with newly formed trabecular bone around the middle body of the fixture.

Histomorphometric analysis of %BIC and %BD was shown in Table 9. The %BIC of separable implant was 68% and that of the non-separable implant was 50% in 3 weeks of healing, and 63% and 59% respectively in 6 weeks of healing. The %BD of the separable implant was 60% and that of the non-separable implant was 64% in 3 weeks of healing, and 60% and 74% respectively in 6 weeks of healing. Quantification of %BIC showed a higher degree of osseointegration and there was no noticeable difference in osseointegration between separable and non-separable implant.

IV. Discussion

In the biomechanical study, finite element analysis was only performed to compare non-separable and separable implant with a single tooth model under static loading. However, since complex and fatigue loading on teeth is important, it is necessary to analyze characteristics and fracture patterns of fatigue between non-separable and separable implant under clinical fatigue loading condition in the actual implant system. As the PVMS values of abutment screw are significantly lower in the separable implant, a possibility of abutment screw fatigue fracture in the fixture is considered lower in separable implant than in non-separable implant. Further evaluation about fatigue loading and fatigue fracture I s needed to explore an influence of fatigue under a long-term repeated loading. Fatigue testing of implant that has new design or technological characteristics can be conducted according to Organization for International Standardization (ISO) protocol 14801 which is one of the mechanical testing guidelines set by Food and Drug Administration[18].

Albrektsson et al. reported six factors to achieve successful osseointegration. There are biocompatibility, design and surface condition of implant, state of implant surgical bed, surgical method, and loading control in healing period are suggested[19]. Therefore, we assessed the difference in osseointegration due to new design of separable implant.

In present animal study, two different designs of implants were tested in the tibia of the rabbit. Apart from being inexpensive, the rabbit model is advantageous in terms of standardization of experiment conditions, fast bone turnover rate and fast skeletal changes[20,21]. Wang et al. reported that there are some similarities between rabbit and human in terms of bone mineral density (BMD) and fracture toughness of mid-

diaphysis[22]. Rabbit is the smallest animal that can accept commercially available dental implants in long bones such as tibia and femur. Therefore, it serves as a good animal model study for evaluating newly designed implant before a clinical study is performed. Following this study performed in a rabbit, a planned preclinical study using a beagle dog model under loading condition with peri-implantitis is in process. Current study based on rabbit tibia model focuses more on the biomechanical stability measuring ISQ, bone volume fraction, RTV, and histological response to evaluate the newly designed separable implant. This study demonstrated a separable implant that offers equal or even better results when compared with the conventional non-separable implant. Particularly during initial healing stages.

Removal torque test and histomorphometric analysis can provide reliable data on the strength of bone–implant interface and quality of anchorage between implant and bone[23], but these destructive assessments are only applicable in an experimental environment. Therefore, RFA was required to predict implant stability in clinical settings. RFA was reported to be a reliable and accurate method for early assessment of implant stability which is related to the bone–implant interface[24].

ISQ measured by resonance frequency instrument reflects the stiffness of bone–implant interface[25,26]. Several factors influencing resonance frequency of implant have been proposed. Factors such as implant design and length, the location of first bone contact, the thickness of cortical bone, trabecular pattern of alveolar bone, bone density and %BIC have been investigated in different model studies including animal experiments and human studies[17,25,27-29].

A different thickness of cortical bone might affect initial ISQ under same fixtures and same surgical experts. Miyamoto et al. found a strong linear correlation between ISQ

and the thickness of cortical bone measured in CT[8]. A rabbit tibia is composed of about 2 mm thickness of cortical bone surrounding a medullar cavity. The separable junction of a separable fixture should be positioned in same bone quality, not to sink in a marrow cavity to standardize the experiment conditions. Therefore, implants should be considered to be installed into a proximal condyle, and not into the long bone. As the location of implant in tibia may influence osseointegration due to different bone features from epiphysis to diaphysis, the implants used in this study were located in sponge bone so the whole fixture surface had similar characteristics of contact bone.

It has been reported an increase of implant stability values measured by RFA device during the healing period in rabbit tibia and human clinical studies[26,30-32]. The results of this study agree with previous studies, indicating that secondary implant stability increased significantly over the 6 weeks of healing period ($p=0.000$). Two-way ANOVA showed that the main effect of healing period on ISQ was significant. Bonferroni's multiple comparison showed that ISQ of 6 weeks (62.84 ± 0.29) was higher than that of 3 weeks (59.20 ± 0.33). In other literatures, rabbits were sacrificed mainly at 4 or 8 weeks for implant evaluation in rabbit tibia model[33-35]. But in this study, rabbits were observed in 3 and 6 weeks to evaluate primary stability and osseointegration since the location of implant placement was condyle metaphysis except cavity, which is considered to have a large impact on osseointegration. In another study, there was a tendency of a difference after 5 days ($p=0.06$) in ISQ measurements with titanium implants placed in tibia of lop-eared rabbits after 5, 14, and 28 days[36].

Percent BIC is one of the predictors of implant stability and initial ISQ was significantly correlated with %BIC. So, RFA is a useful clinical method to predict %BIC, namely the degree of osseointegration, and to evaluate implant stability[37]. But a rough implant surface is covered easily by a thin layer of bone, which does not provide much

support for biomechanical stability. In this case, %BIC usually shows good results. Johansson showed biomechanical test was more sensitive for predicting implant stability than histomorphometric analyses[38]. Therefore, histomorphometric analyses were not statistically processed in this study at first. But after confirmation of separable implant stability with RFA, μCT, and removal torque test in this study, statistics of histomorphometric analysis are planned to proceed.

The most important factor to shorten treatment period is to obtain and maintain osseointegration early. Quantification of %BIC indicates a degree of osseointegration. In a previous study, the mean %BIC value of SLA treated implant placed in proximal tibial metaphysis was 29% in total length of the implant surface after a healing period of 4 weeks[33]. Calvo-Guirado et al. reported that mean %BIC values were 23-40% of four different modified SLA surfaced implants placed in proximal tibial metaphysis after a healing period of 2-8 weeks[34]. The results of this study showed higher %BIC compared to the previous literature.

The RTV results demonstrated significant differences between two implant types ($p=0.000$). Separable implants had significantly higher RTVs than non-separable implants at both 3 and 6 weeks of healing, with no significant difference between the healing periods ($p=0.374$). Separable implant (25.65 ± 1.95) demonstrated 188% higher mean RTV than non-separable implant (13.63 ± 2.24). These results indicated that separable implant markedly improved mechanical fixation of the implant to the surrounding bony structure. It is considered that bone adhesion in the micro gap of a separable implant allowed higher RTVs by increasing bone–implant contact area. Because the gap widened contact area with bone, osseointegration is more likely to occur although exterior design of both implants is identical at first. The gap in separable implant was considered occurred because cover screw was not completely tightened. So,

additional in vivo experiment was performed with separable implants to solve the gap. It was confirmed that there was no gap in separable implant in the additional histology analysis (Figure 15). Structure difference of the gap between the two groups is solved so it is considered that RTV would not be significantly different between separable and non-separable implant with these additional specimens. And the additional experiment is needed for removal torque test to evaluate RTV.

This study assessed biomechanical stability and osseointegration parameters of the newly designed separable implant in rabbit tibia to determine whether separable implant would further improve or interrupt implant stability compared with conventionally available non-separable implant. Based on this evaluation, the separable implant is scientifically documented and the results suggest that separable implant has sufficient osseointegration and biomechanical stability. Side effects or functional impairment was not found in separable implant compared to non-separable implant and safety was also observed. This study showed a separable implant with primary stability, although it has a limitation that the experiment was conducted in rabbit tibia without loading. Although considerable variations may happen after loading of implant prosthetics, this study seems to be suitable to observe initial stability. It is, therefore, necessary to study long term stability of separable implant under clinically loading condition in a future clinical study. Within the limited condition of this study, the results indicate that separable implant may be effective in easily treating peri-implantitis along with the comparable osseointegration and implant stability.

V. Conclusion

In the biomechanical study with finite element model, the newly designed separable implant showed a more excellent load distribution and stress transfer within the bone compared to non-separable implant. Therefore, this proves that there is a lower stress level compared to non-separable implant. There were no significant differences between both current and conventional implants in implant stability and bone volume fraction observed in the preclinical study with rabbit tibia model. However, greater values of removal torque have been observed in the separable implant in relation to the control. This study has therefore demonstrated no significant differences when comparing between separable and non-separable implant. Based on this evaluation, separable implant is scientifically documented and the results suggest that separable implant has sufficient osseointegration and biomechanical stability.

With this, the conclusion of this study is that there is a feasibility of clinical application of separable dental implant fixture based on the osseointegration and biomechanical stability.

Reference

1. Berglundh T, Persson L, Klinge B. A systematic review of the incidence of biological and technical complications in implant dentistry reported in prospective longitudinal studies of at least 5 years. *J Clin Periodontol.* 2002;29 Suppl 3:197-212; discussion 232-193.
2. Derks J, Tomasi C. Peri-implant health and disease. A systematic review of current epidemiology. *J Clin Periodontol.* 2015;42 Suppl 16:S158-171.
3. Atieh MA, Alsabeeha NH, Faggion CM, Jr., Duncan WJ. The frequency of peri-implant diseases: a systematic review and meta-analysis. *J Periodontol.* 2013;84(11):1586-1598.
4. Belibasakis GN. Microbiological and immuno-pathological aspects of peri-implant diseases. *Arch Oral Biol.* 2014;59(1):66-72.
5. Smeets R, Henningsen A, Jung O, Heiland M, Hammacher C, Stein JM. Definition, etiology, prevention and treatment of peri-implantitis - a review. *Head Face Med.* 2014;10:34.
6. Smiler D, Soltan M. The bone-grafting decision tree: a systematic methodology for achieving new bone. *Implant Dent.* 2006;15(2):122-128.
7. Throckmorton GS, Buschang PH, Ellis E, 3rd. Improvement of maximum occlusal forces after orthognathic surgery. *J Oral Maxillofac Surg.* 1996;54(9):1080-1086.
8. Miyamoto I, Tsuboi Y, Wada E, Suwa H, Iizuka T. Influence of cortical bone thickness and implant length on implant stability at the time of surgery-clinical, prospective, biomechanical, and imaging study. *Bone.* 2005;37(6):776-780.
9. Ha SR. Biomechanical three-dimensional finite element analysis of monolithic zirconia crown with different cement type. *J Adv Prosthodont.* 2015;7(6):475-483.

10. Rho JY, Ashman RB, Turner CH. Young's modulus of trabecular and cortical bone material: ultrasonic and microtensile measurements. *J Biomech.* 1993;26(2):111-119.
11. Zhang G, Yuan H, Chen X, Wang W, Chen J, Liang J, Zhang P. A three-dimensional finite element study on the biomechanical simulation of various structured dental implants and their surrounding bone tissues. *Int J Dent.* 2016;2016:4867402.
12. Foley J, Dodson J, Schmidt M, Gillespie P, Besonia Y. *High-bandwidth measurement and validation of bar and plate dynamics.* Air Force Research Laboratory, Munitions Directorate, Eglin AFB, FL 2008.
13. Brizuela-Velasco A, Perez-Pevida E, Jimenez-Garrudo A, Gil-Mur FJ, Manero JM, Punset-Fuste M, Chavarri-Prado D, Dieguez-Pereira M, Monticelli F. Mechanical characterisation and biomechanical and biological behaviours of Ti-Zr binary-alloy dental implants. *Biomed Res Int.* 2017;2017:2785863.
14. Ao J, Li T, Liu Y, Ding Y, Wu G, Hu K, Kong L. Optimal design of thread height and width on an immediately loaded cylinder implant: A finite element analysis. *Comput Biol Med.* 2010;40(8):681-686.
15. Chun HJ, Cheong SY, Han JH, Heo SJ, Chung JP, Rhyu IC, Choi YC, Baik HK, Ku Y, Kim MH. Evaluation of design parameters of osseointegrated dental implants using finite element analysis. *J Oral Rehabil.* 2002;29(6):565-574.
16. Yang J, Xiang HJ. A three-dimensional finite element study on the biomechanical behavior of an FGBM dental implant in surrounding bone. *J Biomech.* 2007;40(11):2377-2385.

17. Sennerby L, Meredith N. Implant stability measurements using resonance frequency analysis: biological and biomechanical aspects and clinical implications. *Periodontol 2000.* 2008;47:51-66.

18. Lee CK, Karl M, Kelly JR. Evaluation of test protocol variables for dental implant fatigue research. *Dent Mater.* 2009;25(11):1419-1425.

19. Albrektsson T, Branemark PI, Hansson HA, Lindstrom J. Osseointegrated titanium implants: Requirements for ensuring a long-lasting, direct bone-to-implant anchorage in man. *Acta Orthop Scand.* 1981;52(2):155-170.

20. Li Y, Chen SK, Li L, Qin L, Wang XL, Lai YX. Bone defect animal models for testing efficacy of bone substitute biomaterials. *J Orthop Translat.* 2015;3(3):95-104.

21. Castaneda S, Largo R, Calvo E, Rodriguez-Salvanes F, Marcos ME, Diaz-Curiel M, Herrero-Beaumont G. Bone mineral measurements of subchondral and trabecular bone in healthy and osteoporotic rabbits. *Skeletal Radiol.* 2006;35(1):34-41.

22. Wang X, Mabrey JD, Agrawal CM. An interspecies comparison of bone fracture properties. *Biomed Mater Eng.* 1998;8(1):1-9.

23. Szmukler-Moncler S, Piattelli A, Favero GA, Dubruille JH. Considerations preliminary to the application of early and immediate loading protocols in dental implantology. *Clin Oral Implants Res.* 2000;11(1):12-25.

24. Heo S, Sennerby L, Odersjö M, Granström G, Tjellström A, Meredith N. Stability measurements of craniofacial implants by means of resonance frequency analysis. A clinical pilot study. *J Laryngol Otol.* 1998;112(6):537-542.

25. Meredith N, Alleyne D, Cawley P. Quantitative determination of the stability of the implant-tissue interface using resonance frequency analysis. *Clin Oral Implants Res.* 1996;7(3):261-267.

26. Sim CP, Lang NP. Factors influencing resonance frequency analysis assessed by Osstell mentor during implant tissue integration: I. Instrument positioning, bone structure, implant length. *Clin Oral Implants Res.* 2010;21(6):598-604.

27. Alsaadi G, Quirynen M, Michiels K, Jacobs R, van Steenberghe D. A biomechanical assessment of the relation between the oral implant stability at insertion and subjective bone quality assessment. *J Clin Periodontol.* 2007;34(4):359-366.

28. Schliephake H, Sewing A, Aref A. Resonance frequency measurements of implant stability in the dog mandible: experimental comparison with histomorphometric data. *Int J Oral Maxillofac Surg.* 2006;35(10):941-946.

29. Nkenke E, Hahn M, Weinzierl K, Radespiel-Troger M, Neukam FW, Engelke K. Implant stability and histomorphometry: a correlation study in human cadavers using stepped cylinder implants. *Clin Oral Implants Res.* 2003;14(5):601-609.

30. Meredith N, Shagaldi F, Alleyne D, Sennerby L, Cawley P. The application of resonance frequency measurements to study the stability of titanium implants during healing in the rabbit tibia. *Clin Oral Implants Res.* 1997;8(3):234-243.

31. Huang HM, Chiu CL, Yeh CY, Lin CT, Lin LH, Lee SY. Early detection of implant healing process using resonance frequency analysis. *Clin Oral Implants Res.* 2003;14(4):437-443.

32. Zhou W, Han C, Yunming L, Li D, Song Y, Zhao Y. Is the osseointegration of immediately and delayed loaded implants the same?-comparison of the implant

stability during a 3-month healing period in a prospective study. *Clin Oral Implants Res.* 2009;20(12):1360-1366.

33. Kim H, Choi SH, Ryu JJ, Koh SY, Park JH, Lee IS. The biocompatibility of SLA-treated titanium implants. *Biomed Mater.* 2008;3(2):025011.

34. Calvo-Guirado JL, Satorres M, Negri B, Ramirez-Fernandez P, Mate-Sanchez de Val JE, Delgado-Ruiz R, Gomez-Moreno G, Abboud M, Romanos GE. Biomechanical and histological evaluation of four different titanium implant surface modifications: an experimental study in the rabbit tibia. *Clin Oral Investig.* 2014;18(5):1495-1505.

35. Yildiz A, Esen E, Kurkcu M, Damlar I, Daglioglu K, Akova T. Effect of zoledronic acid on osseointegration of titanium implants: an experimental study in an ovariectomized rabbit model. *J Oral Maxillofac Surg.* 2010;68(3):515-523.

36. Sennerby L, Gottlow J, Rosengren A, Flynn M. An experimental evaluation of a new craniofacial implant using the rabbit tibia model: Part II. Biomechanical findings. *Otol Neurotol.* 2010;31(5):840-845.

37. Park IP, Kim SK, Lee SJ, Lee JH. The relationship between initial implant stability quotient values and bone-to-implant contact ratio in the rabbit tibia. *J Adv Prosthodont.* 2011;3(2):76-80.

38. Johansson CB, Han CH, Wennerberg A, Albrektsson T. A quantitative comparison of machined commercially pure titanium and titanium-aluminum-vanadium implants in rabbit bone. *Int J Oral Maxillofac Implants.* 1998;13(3):315-321.

VII. Tables

Table 1. Mechanical properties of implant, crown, and bone in finite element models.

Components	Material	Young's modulus (MPa)	Poisson`s ratio
Fixture	Ti-grade 4	105,000	0.34
Abutment	Ti-grade 5	114,000	0.33
Abutment screw	Ti-grade 5	114,000	0.33
Crown	Zirconia	205,000	0.19
Bones	Cortical bone	13,000	0.30
	Cancellous bone	690	0.30

For finite element analysis, Young's modulus and Poisson's ratio were input into the program.

Table 2. Number of elements and nodes in the finite element model.

Components	Elements		Nodes	
	Separable	**Non-separable**	**Separable**	**Non-separable**
Fixture	48692 (up) 104432 (down)	125966	12300 (up) 23594 (down)	24396
Abutment	88637		88637	
Abutment screw	60588		60588	
Crown	121740		121740	
Cortical bone	295533	287389	64492	629174
Cancellous bone	273597	275822	56765	57108

A mesh is composed of nodes and elements.

Meshed models were formed using Hypermesh program.

Table 3. Finite element analysis results of cortical and cancellous bone. The PVMS values were compared between separable and non-separable implants. The PVMS value of cortical bone was around 26% higher in separable implant (138MPa) than in non-separable implant (109MPa) under vertical loading condition, but at oblique load it was around 16% (15 degrees), 20% (45 degrees) lower in separable implant than in non-separable implant. In cancellous bone, separable implant generated higher stress than non-separable implant at all loading conditions.

Direction of load	**Peak von Mises stress (MPa)**			
	Cortical bone		**Cancellous bone**	
	Separable	**Non-separable**	**Separable**	**Non-separable**
100N (axial)	138	109	68	54
100N (15 deg.)	187	223	78	50
30N (45 deg.)	146	182	61	40

Table 4. Finite element analysis results of fixture, abutment, and abutment screw. The PVMS values were compared between separable and non-separable implants. The PVMS values of implant (fixture, abutment, and abutment screw) were higher in separable implant than in non-separable implant at vertical loading condition, but separable implant was rather lower than non-separable implant at oblique loading conditions. In particular, the difference of PVMS between the two groups was significant at oblique load, and the stress values of non-separable fixture were higher than the yield strength (552 MPa) of Titanium grade 4.

Direction of load	**Peak von Mises stress (MPa)**					
	Fixture		**Abutment**		**Abutment screw**	
	Separable	Non-separable	Separable	Non-separable	Separable	Non-separable
100N (axial)	243	177	138	98	164	162
100N (15 deg.)	395	761	219	596	239	706
30N (45 deg.)	362	909	166	594	194	716

Yield strength of Titanium grade 4 is 552 MPa.

Table 5. Descriptive statistics results of implant stability in synthetic bone model. Within each hole size, separable implants showed higher ISQ than non-separable implants without statistically significant differencesin Ø2.2 and 2.8 mm sized hole.But separable implants (76.0 ± 2.2) showed higher ISQ than non-separable implants (71.0 ± 4.5) in Ø3.3 mm sized hole with significant differences.

Hole size (Ø,mm)	**Fixture**	**Mean**	**N**	**P**
2.2	Separable	66.2± 3.9	12	0.7655
	Non-separable	65.5 ± 4.4	12	
2.8	Separable	73.7 ± 3.3	12	0.1615
	Non-separable	70.3 ± 4.6	12	
3.3	Separable	76.0± 2.2	12	0.0146*
	Non-separable	71.0± 4.5	12	

N: number of samples, *p<0.050

Table 6. Descriptive statistics results of implant stability. Within each healing period, separable implants showed lower ISQ than non-separable implants without statistically significant differences.

Interval	**Fixture**	**Mean**	**N**	**p†**
3weeks	Separable	59.00 ± 2.06	33	0.057
	Non-separable	59.41 ± 1.66	35	
6weeks	Separable	62.20 ± 2.52	47	
	Non-separable	63.48 ± 3.86	42	
p§	0.000*			

N: number of samples, §: effect of healing period in two-way ANOVA, †: effect of fixture type in two-way ANOVA, *p<0.050

Table 7. Descriptive statistics results of % bone volume fraction (% BV/TV) in micro CT. Within each healing period, separable implants showed lower %BVF than non-separable implants without statistically significant differences.

Interval	Fixture	Mean	N	p†
3weeks	Separable	50.25 ± 3.78	36	0.198
	Non-separable	50.60 ±5.07	41	
6weeks	Separable	44.99 ±4.39	44	
	Non-separable	46.62 ±5.92	44	
p§	0.000*			

N: number of samples, §: effect of healing period in two-way ANOVA, †: effect of fixture type in two-way ANOVA, *p<0.050

A cylindrical volume of interest (VOI) with a resolution of 9.945 μm included 0.8 mm around the fixture with a height of 0.9mm from the external platform shoulder of the lower part of separable fixture, which was matched up with the location and area of VOI in non-separable fixture.

Bone volume fraction (BV/TV, bone volume to total volume ratio) was directly calculated in the VOI from the 2D and 3D datasets using CT analyser software.

Table 8. Descriptive statistics results of removal torque values (Ncm). There is a significant difference in mean RTV according to the fixture type, and separable implant (25.65 ± 1.95) shows a greater mean RTV than non-separable implant (13.63 ± 2.24).

Interval	**Fixture**	**Mean**	**N**	**p†**
3weeks	Separable	24.22 ± 10.46	9	0.000*
	Non-separable	12.38 ± 3.66	8	
6weeks	Separable	27.08 ± 11.20	13	
	Non-separable	14.88 ± 6.13	8	
p§	0.374			

N: number of samples, §: effect of healing period in two-way ANOVA, †: effect of fixture type in two-way ANOVA, *p<0.050

Table 9. Histomorphometric analysis of %BIC and %BD. The %BIC of separable implant was 68% and that of non-separable implant was 50% in 3 weeks of healing, and 63% and 59% respectively in 6 weeks of healing. The %BD of separable implant was 60% and that of non-separable implant was 64% in 3 weeks of healing, and 60% and 74% respectively in 6 weeks of healing. There is no noticeable difference in osseointegration between separable and non-separable implant.

Interval	**Fixture**	**%BIC**			**%BD**		
		Implant (mm)	**Bone (mm)**	**Ratio**	**ROI (mm^2)**	**Bone (mm^2)**	**Ratio**
3weeks	Separable	365	247	68%	18,064	1,087	60%
	Non-separable	640	318	50%	46,197	29510	64%
6weeks	Separable	350	211	63%	15,309	9,136	60%
	Non-separable	648	379	59%	48,227	35,649	74%

%BIC: percent bone implant contact; %BD: percent bone density

VIII. Figure Legends

Figure 1. Finite element model and loading conditions. (A) Application of preload of 200N vertically at abutment screw assuming fixated state of fixture and abutment. (B) Application of axial 100N, 100N at 15° and 30N at 45° buccolingual load.

Figure 2. Implants installed in different sized holes (Ø2.2, 2.8, 3.3 mm) in synthetic bone models. (A) ISQ measurement was repeated six times from all quarters respectively. (B) A transducer (Smartpeg) was attached to an implant. A transducer probe (Osstell mentor probe) was held close to SmartPeg but contactless so that the probe tip pointed at small magnet on the top of the SmartPeg with a distance of 2–3 mm during pulsing time.

Figure 3. Clinical photographs of fixtures. (A) Separable fixture, (B) Non-separable fixture.

Figure 4. Three-dimensional CAD model of dental implant system. (A) Separable fixture, (B) Non-separable fixture, (C) Abutment screw, (D) Abutment, and (E) Assembled model of implant system.

Figure 5. Implants installed in rabbit tibia model. One fixture was positioned anteriorly and the other was positioned posteriorly of the medial surface of tibial medial condyle with 8mm gap between the fixtures.

Figure 6. Removal torque test. (A) RTV was measured automatically using a digital torque gauge (MTT03-100). (B) An axis of the torque gauze device was aligned to an axis of an implant with mount to apply axial moments in test.

Figure 7. Stress distribution of cortical and cancellous bones, abutment, fixture, and abutment screw under a vertical loading of 100N (axial). Stress was highest at the

junction of fixture and abutment screw as it is mainly contacted region between fixture and abutment screw. (A) Separable fixture, (B) Non-separable fixture.

Figure 8. Stress distribution of cortical and cancellous bones, abutment, fixture, and abutment screw under an inclined loading of 100N (15°). Stress was highest at the region of bending load applied between fixture and abutment. (A) Separable fixture, (B) Non-separable fixture.

Figure 9. Quantitative comparison of ISQ in synthetic bone model. ISQ is shown according to the different sized implant holes (Ø2.2, 2.8, 3.3 mm) between the two groups. Separable implant shows higher ISQ than non-separable implant and all results show reasonable stability greater than 60. Error bars are standard deviation. *$p<0.050$

Figure 10. Quantitative comparison of ISQ in rabbit tibia model. Within each healing period, non-separable implants showed higher ISQ than separable implants without statistically significant differences. Two-way ANOVA showed that the main effect of healing period on ISQ was significant ($F=68.74$, $p=0.000$). The mean ISQ of 6 weeks healing (62.84 ± 0.29) was 6.15 percent higher than that of 3 weeks healing (59.20 ± 0.33) in both types of implants ($p=0.000$). And no significant difference between separable and non-separable implants was confirmed ($F=3.67$, $p=0.057$). Error bars are standard deviation. *$P<0.050$

Figure 11. Two-dimensional and three-dimensional datasets of micro CT. (A) A cylindrical volume of interest (VOI) with a resolution of 9.945 μm includes 0.8 mm around the fixture with a height of 0.9mm from the external platform shoulder of the bottom part of a separable fixture, which was matched up with the location and area of VOI in a non-separable fixture. New bone formation around the micro gap of a separable fixture is observed. (B) Three-dimensional images of the trabecular bone structures

around the implant could be generated using CTvox program.

Figure 12. Quantitative comparison of BVF in rabbit tibia model. Within each healing period, non-separable implants showed higher BVF than separable implants without statistically significant differences. In comparing BVF with different healing period, mean BVF in 3 weeks of healing (50.43 ± 0.56) was 10.09 percent higher than that in 6 weeks of healing (45.81 ± 0.52) with significant statistic differences ($F=36.38$, $p=0.000$). And no significant difference between separable and non-separable implants was confirmed ($F=1.67$, $p=0.198$). Error bars are standard deviation. *$p<0.050$

Figure 13. Quantitative comparison of removal torque value in rabbit tibia model. There is a significant difference in mean RTV according to the fixture type. Separable implant (25.65 ± 1.95) shows a greater mean RTV than non-separable implant (13.63 ± 2.24). No significant difference depending on the healing period was confirmed ($F=0.81$, $p=0.374$). Error bars are standard deviation. *$P<0.050$.

Figure 14. Histomorphometric analysis of %BD. Percent bone density (%BD) is the percentage of new bone formation area ratio inside threads within region of interest (ROI). The upper threads area was included but the apical area was excluded in ROI of %BD. All the measurements were calculated under 100× magnification. The %BD of separable implant was 60% and that of non-separable implant was 64% in 3 weeks of healing, and 60% and 74% respectively in 6 weeks of healing. (A) ROI of %BD (B) New bone formation area of %BD.

Figure 15. Histologic appearance of separable and non-separable implant at 6 weeks (H&E stained). There is no noticeable difference in osseointegration between two groups. Both sections showed osteoid in woven bone around the fixture, which suggested new bone formation. The fixtures were predominantly in contact with marginal cortical bone

along upper edge of the fixture and in tight contact with newly formed trabecular bone around middle body of the fixture. No prominent inflammation or soft tissue involvement between the bone and the fixture were found. (A, C, E) Separable implant. No bone engagement between the micro gaps of the separable fixture was found at an additional experiment. (B, D, F) Non-separable implant. (A,B 200x; C,D 40x; E,F 10x)

IV. Figures

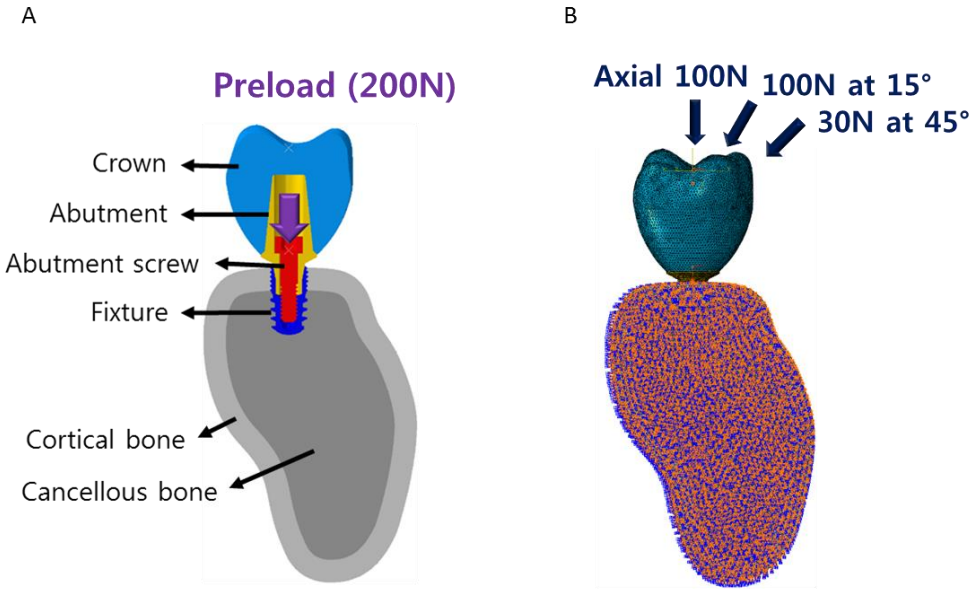

Figure 1.

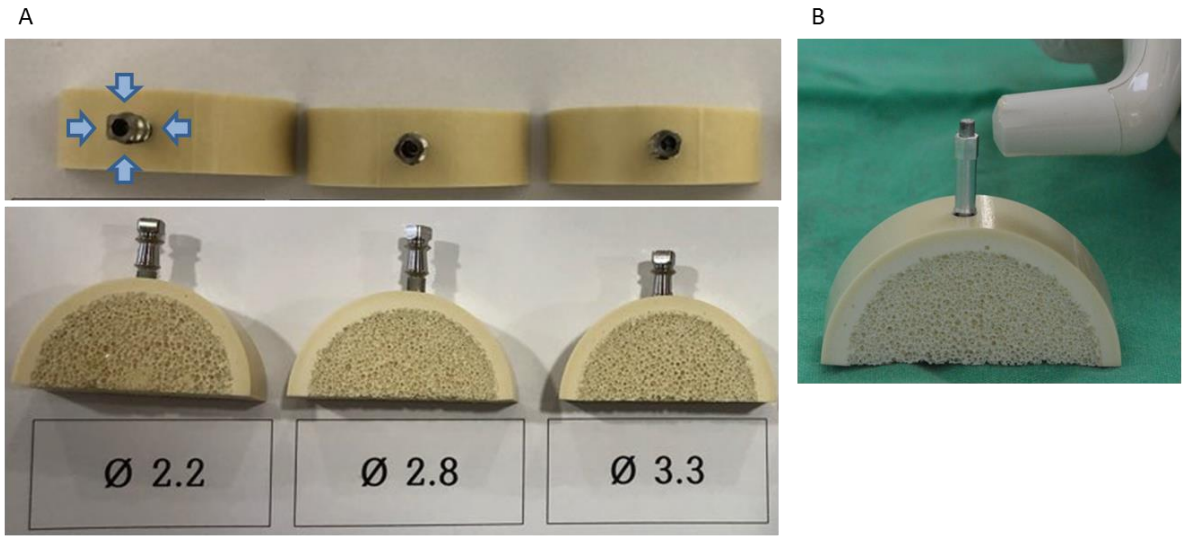

Figure 2.

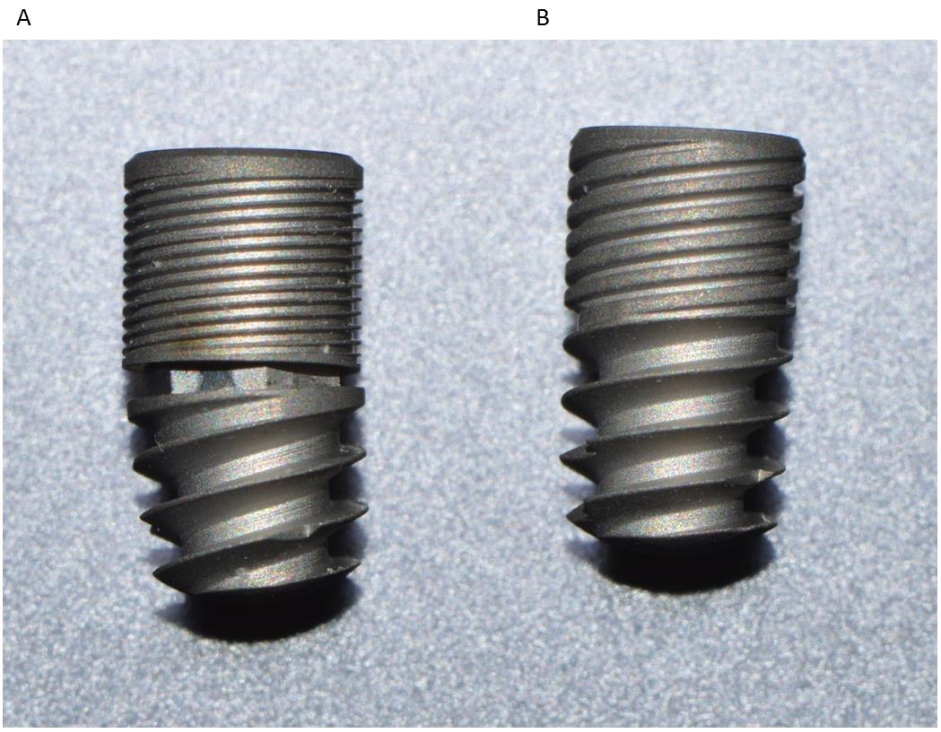

Figure 3.

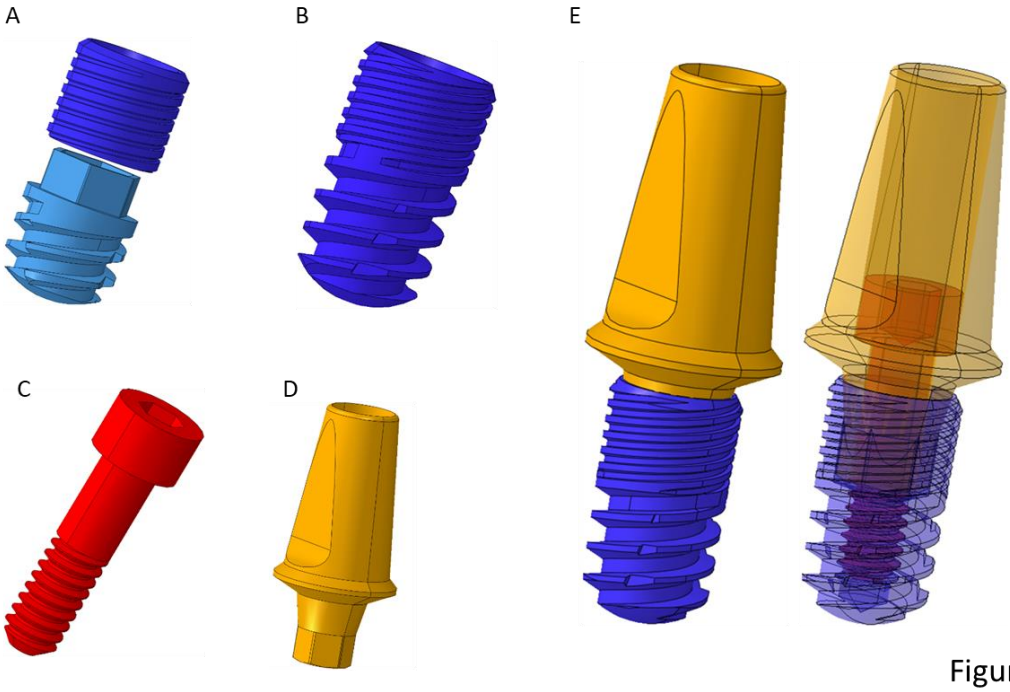

Figure 4.

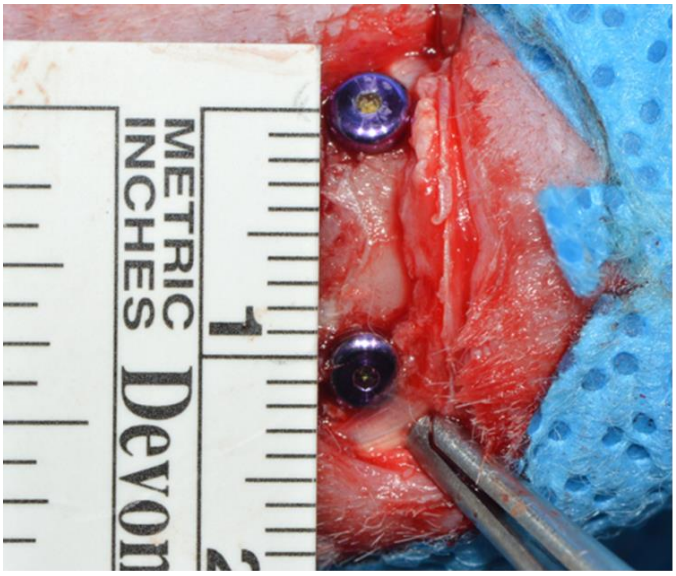

Figure 5.

A

B

Figure 6.

A

B

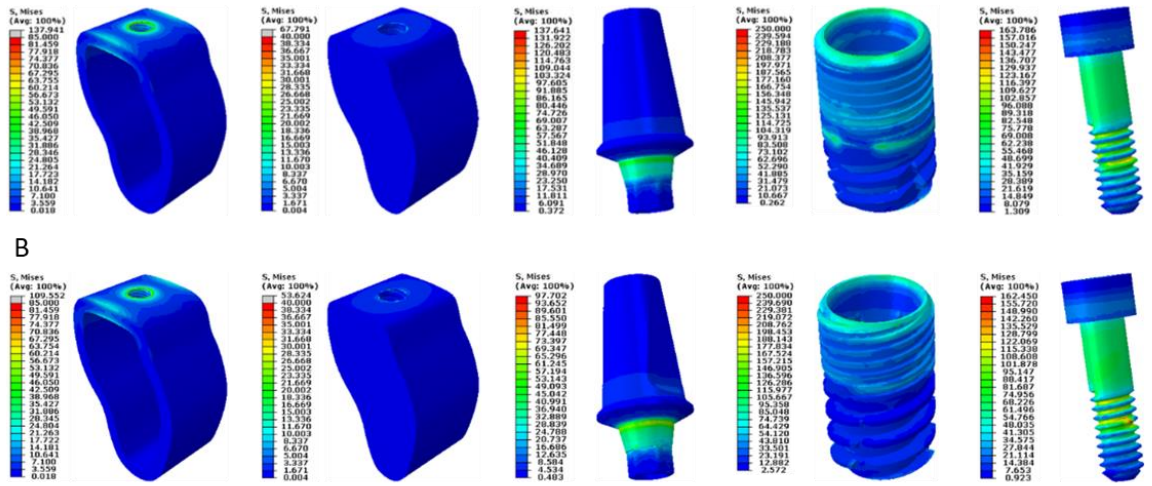

Figure 7.

A

B

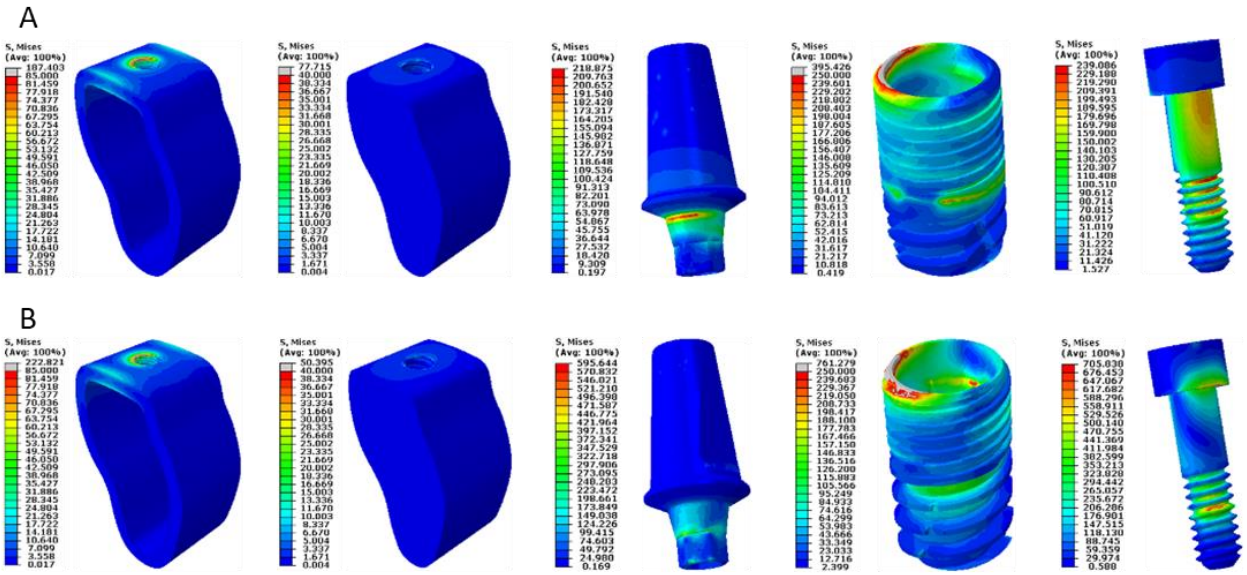

Figure 8.

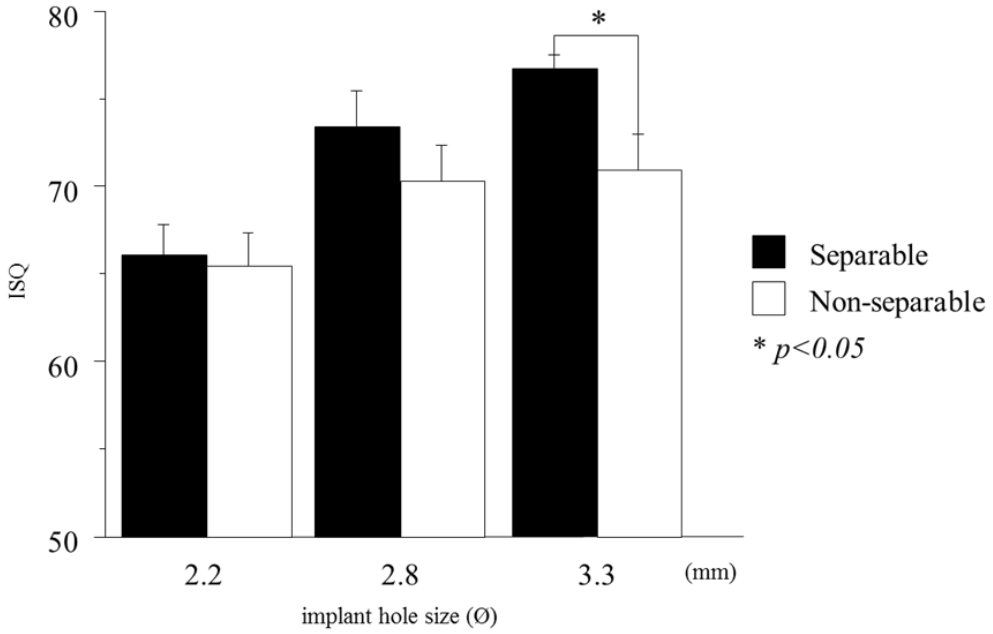

Figure 9.

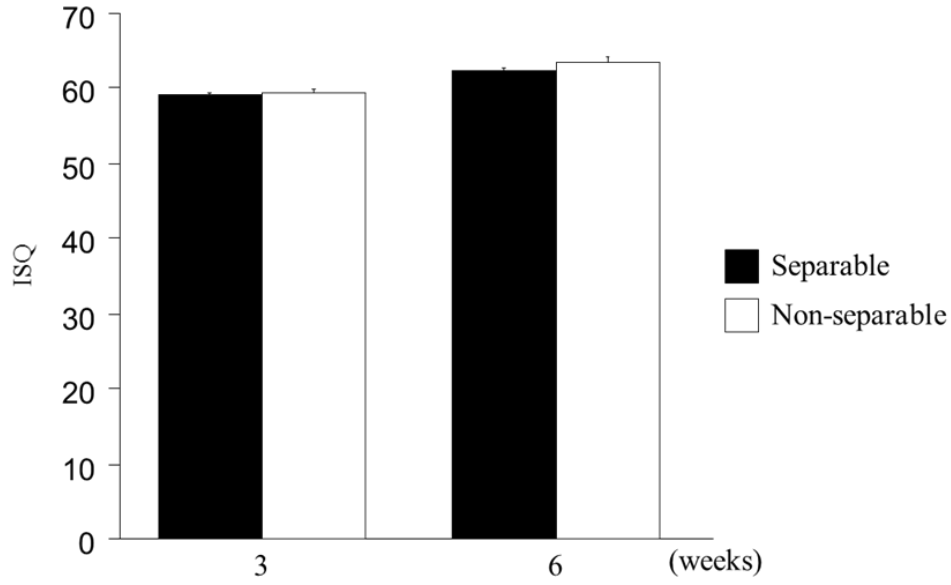

Figure 10.

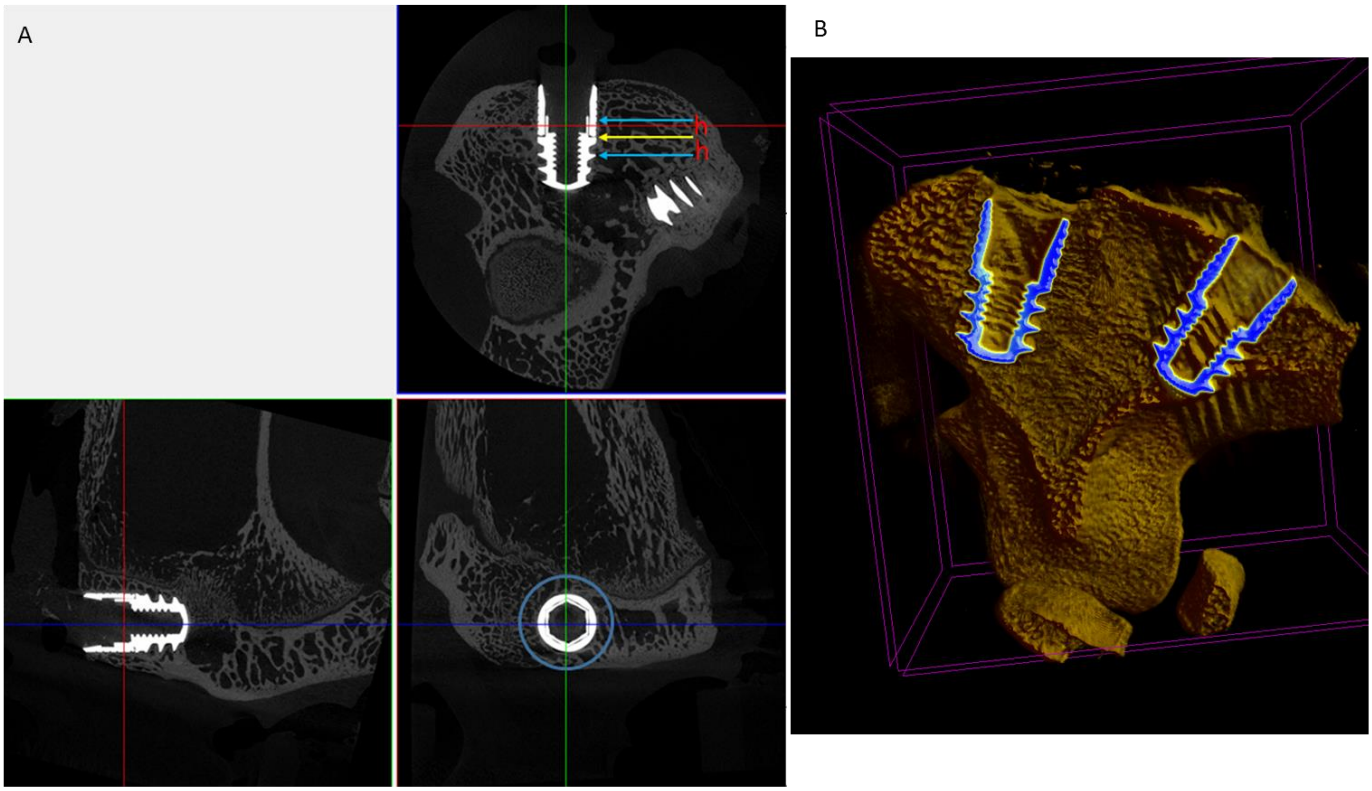

Figure 11.

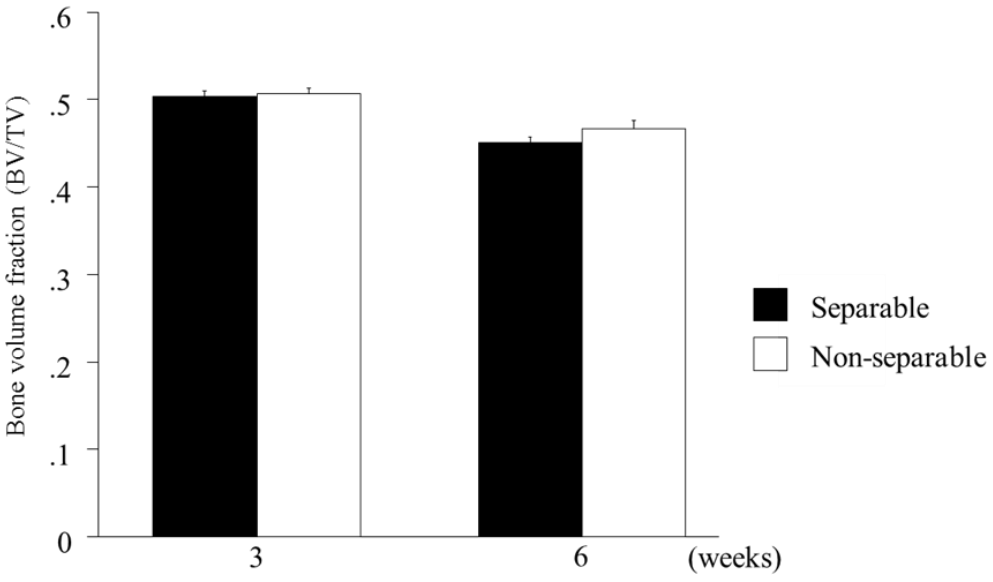

Figure 12.

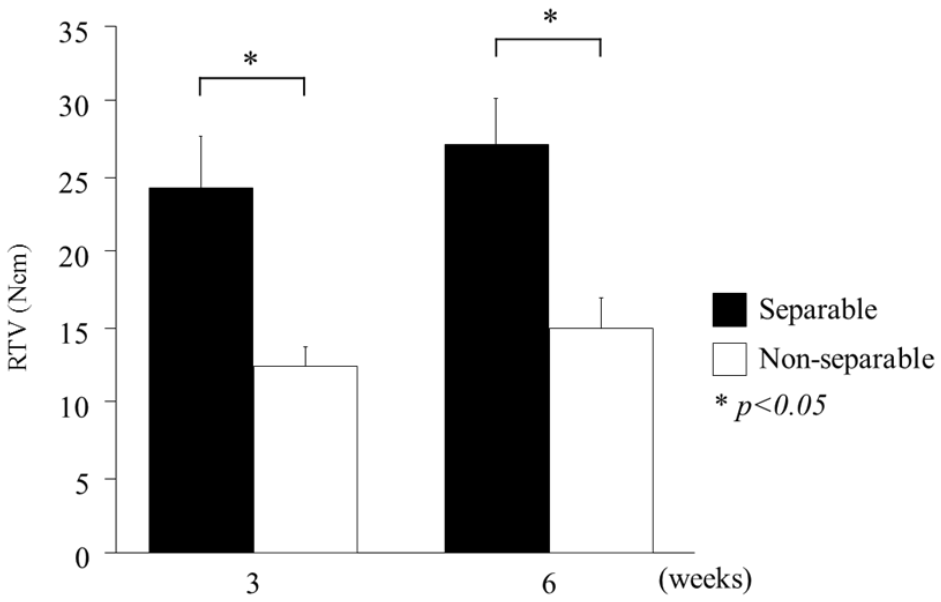

Figure 13.

A

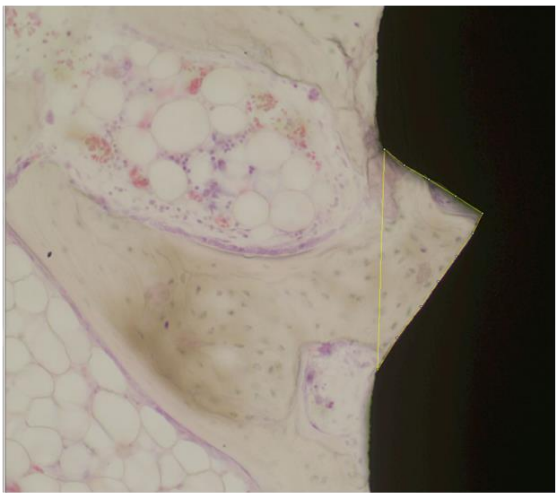

B

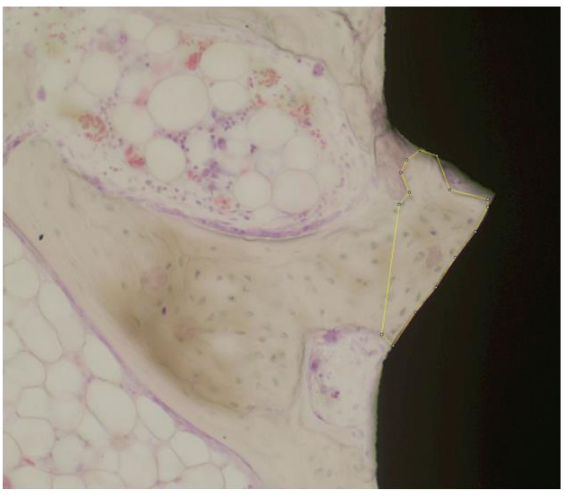

Figure 14.

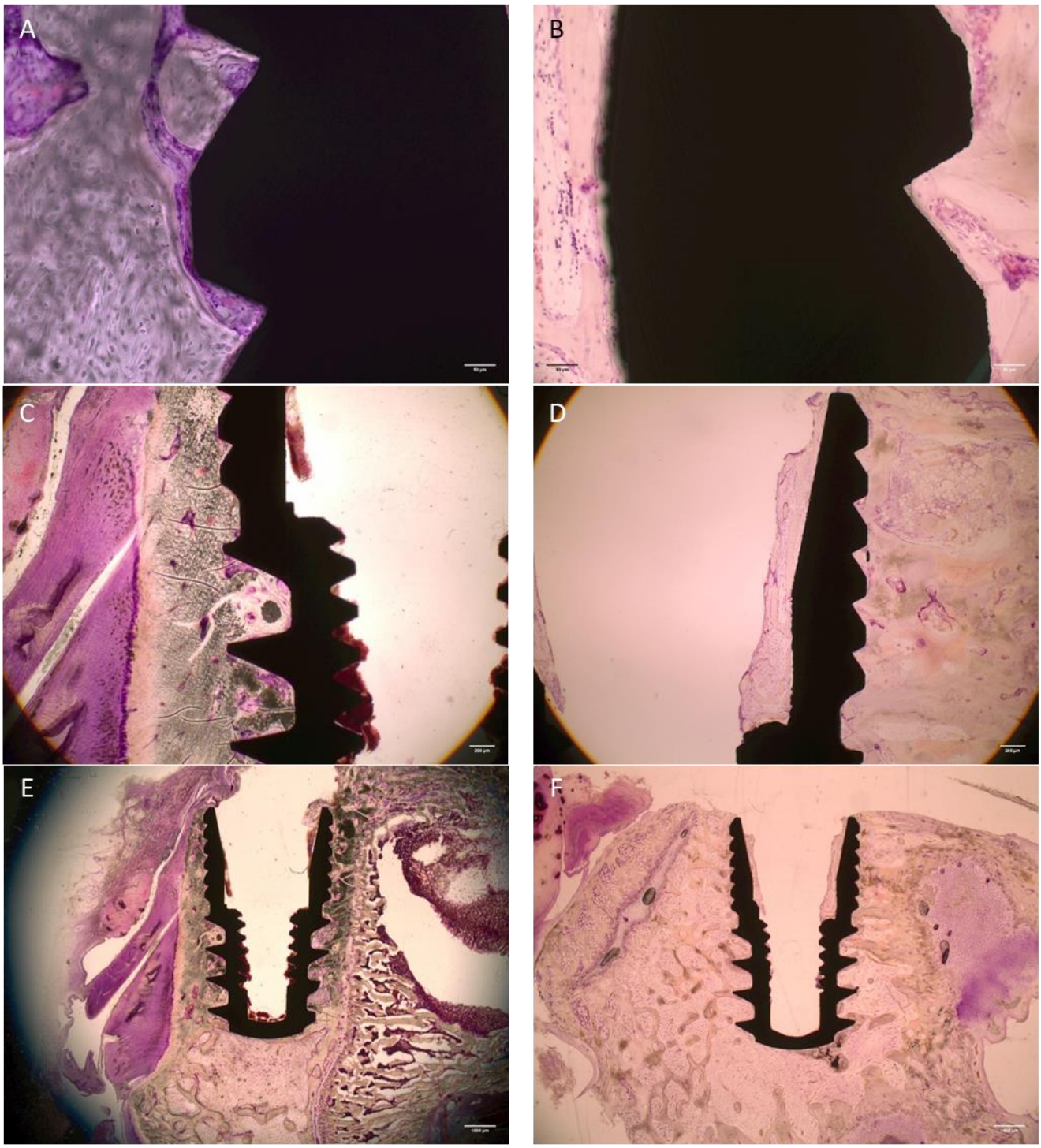

Figure 15.

국문초록

분리형 치과 임플란트 식립체의 생역학 및 전임상 평가

서울대학교 대학원 치의과학과 석사과정 구강악안면외과학 전공

정주희 (Joohee Jeong)

(지도교수 이 종 호)

목 적

임플란트 주위염 처치와 재생치료를 용이하게 할 수 있는 하나의 방법으로 식립체가 상부와 하부로 분리 가능한 치과 임플란트를 새롭게 고안하였다. 진행된 임플란트 주위염에서 치조골 파괴로 임플란트 식립체가 노출된 경우, 건전한 하부 식립체는 유지하면서 노출되어 감염된 상부 식립체 부분만 제거 후 새로운 상부 식립체로 쉽게 교체할 수 있다. 본 연구의 목적은 이렇게 새롭게 디자인된 분리형 임플란트로 임플란트 주위염의 주원인인 세균을 물리적으로 제거하고 염증을 완화하여 완전한 치료를 도모하는 것이다. 새로이 고안된 분리형 임플란트의 임상 적용 타당성을 위해 생체역학적 안정성과 골유

합을 평가하고 비분리형 임플란트와 비교하였다.

방 법

길이 6.0mm, 직경 3.4mm의 형상이 동일한 분리형과 비분리형(일체형) 임플란트 식립체를 제작하였다. 분리형 임플란트 식립체는 기존 상용화 된 일체형 임플란트 식립체가 상하부 두 부분으로 분리가 가능하도록 설계하였다. 분리형과 일체형 임플란트의 생체역학적 분석을 위하여, 컴퓨터 단층촬영 영상을 기반으로 3차원 하악골 유한요소모델을 구축하여 단일 임플란트 식립 모델을 구현하였다. 치아에 수직 방향으로 100N, 수직과 15도로 100N, 수직과 45도로 30N의 하중을 적용하여 비교 분석하였다. 동물 실험에서 총 40마리 토끼의 좌측 경골에는 분리형 임플란트를, 우측 경골에는 일체형 임플란트를 각각 2개씩 식립하였다. 식립 3주, 6주차에 희생하여 공진주파수 분석, 제거 회전력 측정, 미세 컴퓨터 단층촬영 평가, 조직병리학적 평가 및 조직형태계측학적 분석을 시행하였다.

결 과

생체 역학적 분석 시 분리형 임플란트가 일체형 임플란트에 비해 수직 하중에서 악골의 응력이 높게 발생되지만, 해면골에 응력이 더 잘 분산되어 피질골에서의 응력집중 현상은 감소한 것으로 고려되었다. 또한, 분리형 임플란트는 일체형 임플란트에 비해 모든

하중에서 응력분산 효과가 더 양호하여 생체 역학적 안전성이 충분할 것으로 사료된다. 토끼 경골 임플란트 식립 모델에서 임상적으로 양호한 치유 과정을 통해 연조직의 밀폐와 경조직의 골유착, 임플란트 초기 성공을 관찰하였다. 임플란트 안정성 지수와 방사선학적 평가에서 분리형 임플란트와 일체형 임플란트는 3주차와 6주차 모두 유의한 차이를 보이지 않았으며, 제거 회전력 평가에서 분리형 임플란트가 일체형 임플란트에 비해 3주차와 6주차 모두 유의하게 높은 결과 값을 보였다. 본 연구의 결과 분리형 임플란트의 안정성을 확인하였으며 임상 적용 가능성을 보여주었다.

주요어: 분리형 식립체, 치과 임플란트, 생체역학, 골유합, 안정성

학번: 2017-22467